CH2011 Extension Series No. 2

Climate scenarios of seasonal means: extensions in time and space

Andreas M. Fischer [1], Mark Liniger [1], Christof Appenzeller [1, 2]

[1] Federal Office of Meteorology and Climatology MeteoSwiss, Switzerland

[2] Center for Climate Systems Modeling (C2SM), Switzerland

C2SM Center for Climate Systems Modeling

Schweizerische Eidgenossenschaft
Confédération suisse
Confederazione Svizzera
Confederaziun svizra

Swiss Confederation

Federal Department of Home Affairs FDHA
Federal Office of Meteorology and Climatology MeteoSwiss

ETH
Eidgenössische Technische Hochschule Zürich
Swiss Federal Institute of Technology Zurich

NCCR CLIMATE
Swiss Climate Research

OcCC
Organe consultatif sur les changements climatiques
Beratendes Organ für Fragen der Klimaänderung

Abstract

At the heart of the CH2011 report, projections for seasonal mean values were derived based on the joint analysis of several regional climate models (RCMs) from the ENSEMBLES project assuming the A1B emission scenario. The projections were obtained with a Bayesian algorithm and disseminated for three different Swiss regions, four seasons and three projection periods in the 21st century. Uncertainty was expressed with three estimates: a lower, a medium and an upper estimate. Projections for the A2 and RCP3PD emission scenario were derived with a scaling approach based on global mean temperature. In the present study, we extend this CH2011 product (i.e., «the climate scenarios of seasonal means») to provide end-users additional climate information in time and in space.

First, the multi-model combination algorithm is applied to two newly defined Alpine regions providing climate change information at higher elevations. With this extension, estimates for climate change can now be provided for entire Switzerland. The resulting projections indicate a weak positive elevation-dependency of temperature increases (i.e., larger temperature changes at higher altitudes) along with a slightly less pronounced summer drying at higher altitudes toward the end of the century.

Second, annual mean changes instead of seasonal averages are presented. For temperature, the scenarios of annual means are close to taking the arithmetic average over the four respective seasonal mean scenarios. They show an increase in temperature toward the end of the century of around 3.8-4.3°C following the A2 scenario and 3.2–3.7°C following the A1B scenario (medium estimates depending on region). For the mitigation scenario RCP3PD, temperatures are expected to rise less strongly: in the mean by only about 1.4–1.6°C. Regarding precipitation, the annual mean changes stay close to zero throughout the century with uncertainty ranges being markedly smaller compared to seasonal averaged quantities.

Third, the multi-model combination is applied to additional future scenario periods complementing the existing ones of CH2011 and providing end-users continuous scenarios of seasonal means. These projections show that temperature mean changes evolve almost linearly over the century following the A1B scenario, while summer precipitation decreases earlier and stronger in the western regions CHAW and CHW compared to the rest of Switzerland. The analysis further shows that internal decadal variability represents an important contributor to uncertainty in the CH2011 scenarios of seasonal means, even for projections at the end of the 21st century.

Reviewers

Reto Knutti (ETH Zurich), Sven Kotlarski (ETH Zurich)

Acknowledgements

Friederike Fröb (MeteoSwiss) is acknowledged for helpful editorial corrections on the manuscript. The ENSEMBLES data used in this work was funded by the EU FP6 Integrated Project ENSEMBLES (Contract number 505539) whose support is gratefully acknowledged.

Recommended citation

Fischer, A. M., M. A. Liniger, and C. Appenzeller, 2015: Climate scenarios of seasonal means: extensions in time and space, *CH2011 Extension Series No. 2,* Zurich, 18 pp.

Addresses

Center for Climate Systems Modeling (C2SM)
ETH Zürich, CHN
Universitätsstrasse 16
CH-8092 Zürich

Institute for Atmospheric and Climate Science
ETH Zürich, CHN
Universitätsstrasse 16
CH-8092 Zürich

Federal Department of Home Affairs FDHA
Federal Office of Meteorology and Climatology MeteoSwiss
Operation Center 1
P.O. Box 257
CH-8058 Zurich-Airport

Download

Extension Article and Scenario Data: www.ch2011.ch

Contact

info@ch2011.ch

The CH2011 climate scenarios of seasonal means are extended in time and space to provide additional climate change information over Switzerland.

In addition to CH2011, the new climate scenario products of temperature and precipitation change comprise: (a) scenarios of seasonal means for two Alpine regions, (b) scenarios of annual averages and (c) scenarios of seasonal means at additional future periods.

1| Climate scenarios of seasonal means

In CH2011, expected future changes in temperature and precipitation were presented and disseminated at different spatial and temporal aggregation levels: as seasonal and regional means, as regional means at daily resolution and at the local scale at daily resolution. Here, we revisit the climate scenarios of seasonal means (Chapter 3 of CH2011 2011). These projections were based on the joint analysis of several regional climate models (RCMs) driven at their boundaries by global climate models (GCMs). The RCMs (obtained from the EU FP6 ENSEMBLES project) were all run assuming the A1B emission scenario (Nakicenovic and Swart, 2000) at a common model resolution of 25 km by 25 km. Since those RCMs driven by the same GCMs are highly correlated, they were averaged beforehand. In total, eight averaged RCM-GCM simulations were considered up to 2050, while a reduced set of six averaged simulations provided the basis for the assessment after 2050.

The model-data were spatially aggregated to three equally spaced regions: northeastern Switzerland («CHNE»), western Switzerland («CHW») and Switzerland south of the Alps («CHS»). Furthermore, the model projections were seasonally aggregated and their changes analyzed at three future 30-year-long periods: 2020–2049, 2045–2074, and 2070–2099. For simplicity these scenario periods are addressed with the respective central year of the time window, i.e. «2035», «2060», and «2085». The respective changes in temperature and precipitation for these periods were computed with respect to the common reference period 1980–2009 («1995»).

Generally, individual climate model projections diverge significantly from each other resulting in different potential responses to the increase in atmospheric greenhouse gas concentrations. To quantify this kind of uncertainty, a sophisticated multi-model combination algorithm was employed (Buser et al. 2009; Fischer et al. 2012). The outcome of this procedure is a statistical distribution (probability density function, PDF) of expected climate changes at a future time-period that is consistent with the underlying assumptions and data at hand. Although formally probabilistic, the resulting PDF was only used to derive three percentiles thereof (i.e., the 2.5th, 50th and 97.5th percentiles), which were further interpreted by the CH2011 report as a «lower estimate», «medium estimate», and «upper estimate» without attaching explicit probabilities to them.

The rationale for this procedure was expert judgment by the CH2011 authors that suggested much larger uncertainty levels than actually assessed from the limited model data set used in CH2011 (e.g. Knutti et al. 2010). For more details on the uncertainty framework of CH2011 we refer to Appendix A1 and to Fischer et al. (2012). The joint multi-model assessment with three estimates as outcome was applied to both temperature and precipitation and to each season, region and scenario period separately. In addition, to derive expected changes for non-A1B emission scenarios (i.e., in absence of explicit RCM-GCM simulations), we relied on an established scaling method that allowed us to further extend the climate scenarios to the emission scenarios A2 and RCP3PD.

Since the release of the CH2011 scenarios, the seasonal mean scenarios have been subject to extensions in time and space that target specific end-user needs: in particular this involves a new assessment over two newly defined Alpine regions (Section 2), an additional assessment of annual averages instead of seasonal averages (Section 3), and an assessment over additional future scenario periods complementing the ones from CH2011 (Section 4). In the following, we present the main results of this extension work together with some background on the methodology.

2| Climate Scenarios over Alpine Regions

At the time of writing the CH2011 report, the confidence in the capabilities of simulating Alpine climate with RCMs was not high enough to make clear statements. Therefore, the entire Alpine region had been excluded. However, recent studies explored this issue in greater detail and showed that model simulations over this area are indeed meaningful (Im et al. 2010; Kotlarski et al. 2012). Zubler et al. (2014) consequently extended the CH2011 climate scenarios of seasonal means by two additional higher-elevated regions: western Alps («CHAW») and eastern Alps («CHAE») (see Figure 1, highlighted with a star symbol). As in CH2011 (2011), the regional delineation of the two Alpine regions was based on a combination of expert judgment and pairwise correlations between grid-cells, to yield climatologically homogeneous regions of similar size. Likewise, the application of the joint multi-model combination algorithm over the new regions required conceptually the same methodological procedures as documented in CH2011 (2011).

However, in this article, we present a slightly modified version («version 2.0») to the scenarios described in Zubler et al. (2014). The difference concerns the selection of station observations for calculating internal decadal variability. The new approach primarily affects the uncertainty range of relative precipitation changes. In particular over the region CHAW at winter and spring, version 2.0 features a larger uncertainty range than version 1.0 (see Appendix A2 for more details).

For the A1B emission scenario the multi-model assessment over the Alpine regions shows that seasonal temperatures are subject to a continuous increase over the 21st century with a larger change during summer time (Figure 1). The warming seasonal signals at 2085 with medium estimates of 3.2–4.6°C over the two Alpine regions are slightly higher compared to north and south of the Alpine ridge. In fact, an elevation gradient in surface temperature change has been also found in many other regions of Europe based on the analysis of one RCM-GCM simulation (Kotlarski et al. 2012).

As indicated by the upper and lower estimates in Figure 1, significant deviations from the medium estimates are possible. For A1B at the end of the century these deviations lie around 1°C above or below the medium estimate. Similar to the lowland regions, the influence of a particular emission scenario becomes most prominent at the end of the century: for the RCP3PD scenario seasonal mean temperatures are expected to increase by 1.4–2°C, while seasonal temperature changes for the A2 emission scenario are projected to lie in a range of 3.7–5.3°C (medium estimates depending on season, see Table A1).

Regarding precipitation changes, the assessment over the Alps is qualitatively consistent with the regional projections at lower altitudes (CH2011 2011). Summer precipitation is likely to decrease toward the end of the century with a stronger signal in the western part. Furthermore, there is a tendency for winter precipitation to increase over CHAE, a result that is similar to the projections over the adjacent region of Switzerland south of the Alps (CHS) indicating that similar processes affect the climate over these two regions.

For the summer season and the A1B scenario the projections for 2085 indicate a decrease in the mean of 13% (over CHAE) and of 20% (over CHAW). The magnitude of precipitation decrease depends strongly on the emission scenario: in case of the RCP3PD emission scenario seasonal amounts are expected to decrease by 6–8%, and in case of the A2 scenario by 15–23% (medium estimates depending on region, see Table A2). In their localized scenarios at a 2 x 2 km grid over Switzerland, Zubler et al. (2014) found a tendency for a somewhat reduced summer drying with increasing altitude. This can to some part be explained by larger absolute precipitation amounts at higher altitudes, but is also associated with different precipitation type responses (large-scale precipitation versus convective precipitation) simulated at lower and higher elevated regions (Fischer et al. 2014).

From autumn to spring no common sign of change can be inferred from the multi-model assessment in any of the three emission scenarios (Figure 1 and Table A2). As in case of temperature projections, the upper and lower estimates of seasonal precipitation changes do not rule out the possibility of prominent departures, which often deviate by around +/- 15% from the medium estimate (over CHAE and CHAW).

Figure 1

Projected future changes of temperature (°C, middle row) and relative precipitation changes (%, lower row) for four seasons and five Swiss regions: northeastern Switzerland (CHNE), western Switzerland (CHW), Switzerland south of the Alps (CHS), and the two new regions (marked with a star symbol): eastern Alpine Switzerland (CHAE), and western Alpine Switzerland (CHAW). Projections are for 30-year averages centred at 2035 (blue), 2060 (orange), and 2085 (green) with respect to the reference period 1980–2009 and assuming the A1B emission scenario. The coloured bars span the range between upper and lower estimates, while the thick horizontal lines represent the medium estimates. The crosses mark model-simulated changes as used for the multi-model combination. Tabulated values of the three uncertainty estimates over CHAW and CHAE for the emission scenarios A1B, A2 and RCP3PD can be found in Table A1 and A2. Note, that these estimates are based on version 2.0 of the seasonal mean scenarios over the Alps and differ to those of Zubler et al. (2014).

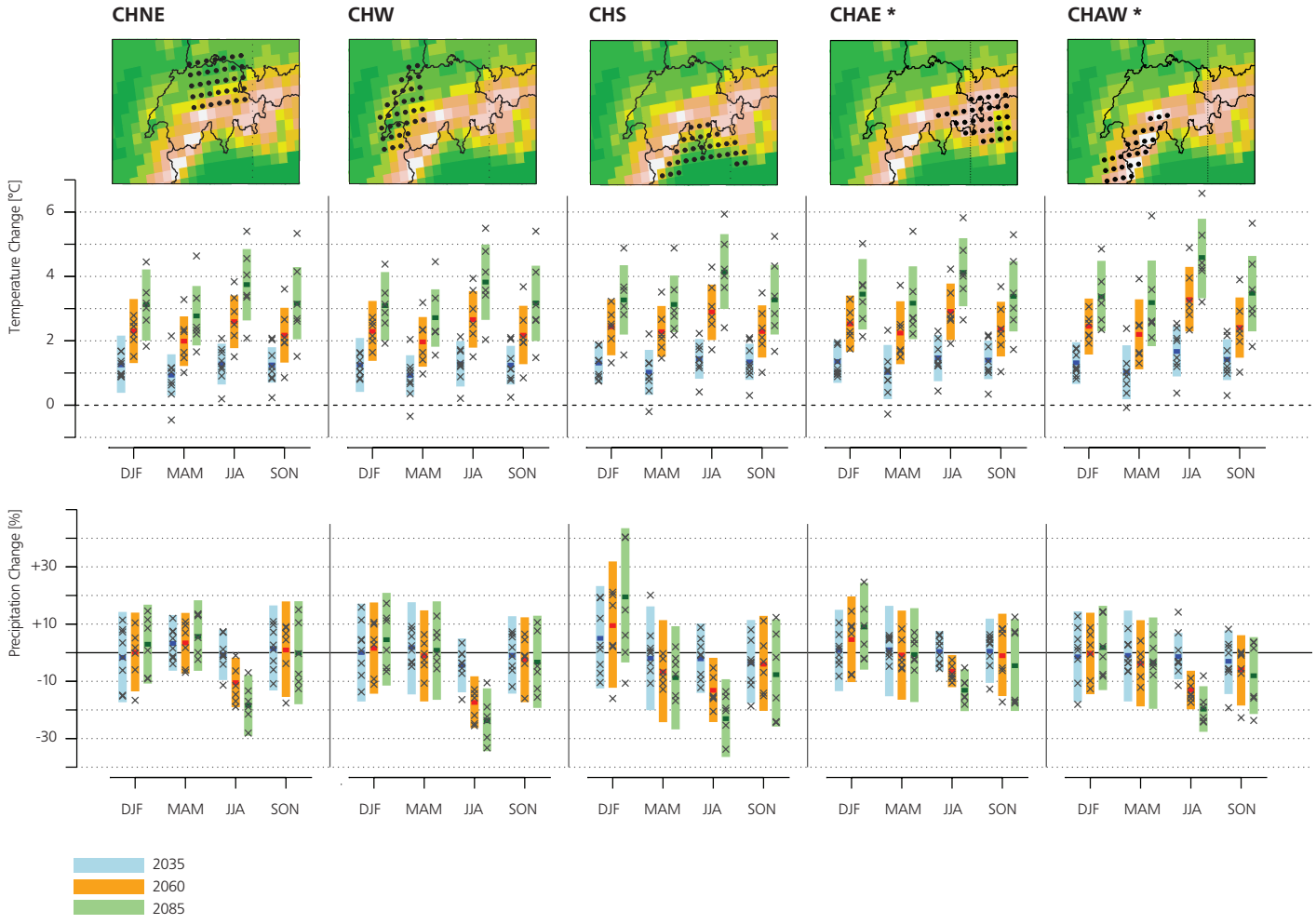

3| Climate scenarios of annual averages

While seasonal mean changes have been described in detail in CH2011, changes of annual averages were not analyzed. Although the decrease in summer precipitation is expected to affect the annual cycle of precipitation over Switzerland toward the end of the century (Bosshard et al. 2011), it remains unclear, whether the drying is strong enough to influence the climate change signal for the annual sum of precipitation. This information is relevant for a number of stakeholders in adaptation planning, particularly those that deal with long-term water storage and water management (FOEN 2012).

Since precipitation changes are expressed in relative terms, a simple average of the scenarios of seasonal means to derive annual mean changes is not valid. But even in case of temperature, depending on the seasonal cycle of modeled changes, such a procedure might not be allowed and must be checked first. Therefore, the CH2011 multi-model combination suite is applied to modeled annual average quantities separately. This requires to revisit the pre- and postprocessing steps that were applied in case of seasonal mean changes (Fischer et al. 2012 and Appendix A1). The multi-model assessment of annual averages is done for the same configurations regarding selection of regions, scenario periods and emission scenarios. The outcome in form of lower, medium and upper estimates is displayed in Figure 2 for the A1B emission scenario and all five sub-regions. In Table A3 and A4 the actual data points can be found together with the estimates following the RCP3PD and A2 scenarios.

Averaged over the full year, temperature according to A1B is expected to steadily rise over the 21st century with medium estimates ranging from 1.2–1.4°C at 2035, 2.3–2.6°C at 2060 and 3.2–3.7°C at 2085 depending on region (Figure 2). From these medium estimates significant deviations are possible as indicated by the lower and upper estimates. At 2085 these deviations often amount to more than +/- 1°C from the medium estimate. No clear distinction between the emission scenarios can be found at 2035, while at later periods this becomes much more evident. Toward the end of the 21st century, temperature is expected to rise by only about 1.4–1.6°C following the RCP3PD emission scenario, while an increase of 3.8–4.3°C is projected if global greenhouse gas emissions evolve as in the A2 scenario (regionally dependent medium estimates).

In contrast to temperature, no robust sign of change can be inferred regarding annual average precipitation. In fact, throughout the 21st century over the whole of Switzerland and considering all emission scenarios, the medium estimates are projected to stay close to zero (Figure 2 and Table A4). Thereby, the uncertainty range between lower and upper estimates is bounded by maximum -12% and +9%. The absence of a common sign of change suggests that the summer decrease in the models is compensated by increases in one or more of the remaining seasons.

How do the scenarios of annual means presented here differ from a simple average of the seasonal mean scenarios over the year? In case of temperature, it indeed turns out that the resulting uncertainty estimates from the two approaches lie close to each other: the medium estimates differ only marginally (around 0.01°C), while the upper (lower) estimates are about 0.2°C higher (lower) in case of averaging the seasonal mean scenarios. The close agreement between the two approaches is an indication that the ranking of model-simulated changes stays relatively similar from season to season. This means for instance that a model with a particularly strong warming in one season likely projects above-average warming in the next season too and vice versa (see Fischer et al. 2016 for more details on the inter-seasonal correlation). Averaging the separately derived seasonal scenarios therefore provides a good approximation of annual mean changes. As mentioned above, in case of relative precipitation, a simple average over the seasons is not allowed. Comparing directly the uncertainties of annual mean changes against those of seasonal mean changes, it turns out that the uncertainty range is considerably lower in case of annual means. This lower uncertainty can be partly explained by internal decadal variability that is substantially smaller for 12-month averages compared to seasonal averages.

Figure 2

Projected future changes of annual averaged temperature (°C, middle row) and precipitation (relative, in %, lower row) for five Swiss regions as in Figure 1. Projections are for 30-year averages centred at 2035 (blue), 2060 (orange), and 2085 (green) with respect to the reference period 1980–2009 and assuming the A1B emission scenario. The colored bars span the range between upper and lower estimates, while the thick horizontal lines represent the medium estimates. The crosses mark model-simulated changes as used for the multi-model combination. Tabulated values of the three uncertainty estimates following the emission scenarios A1B, A2 and RCP3PD can be found in Table A3 and A4.

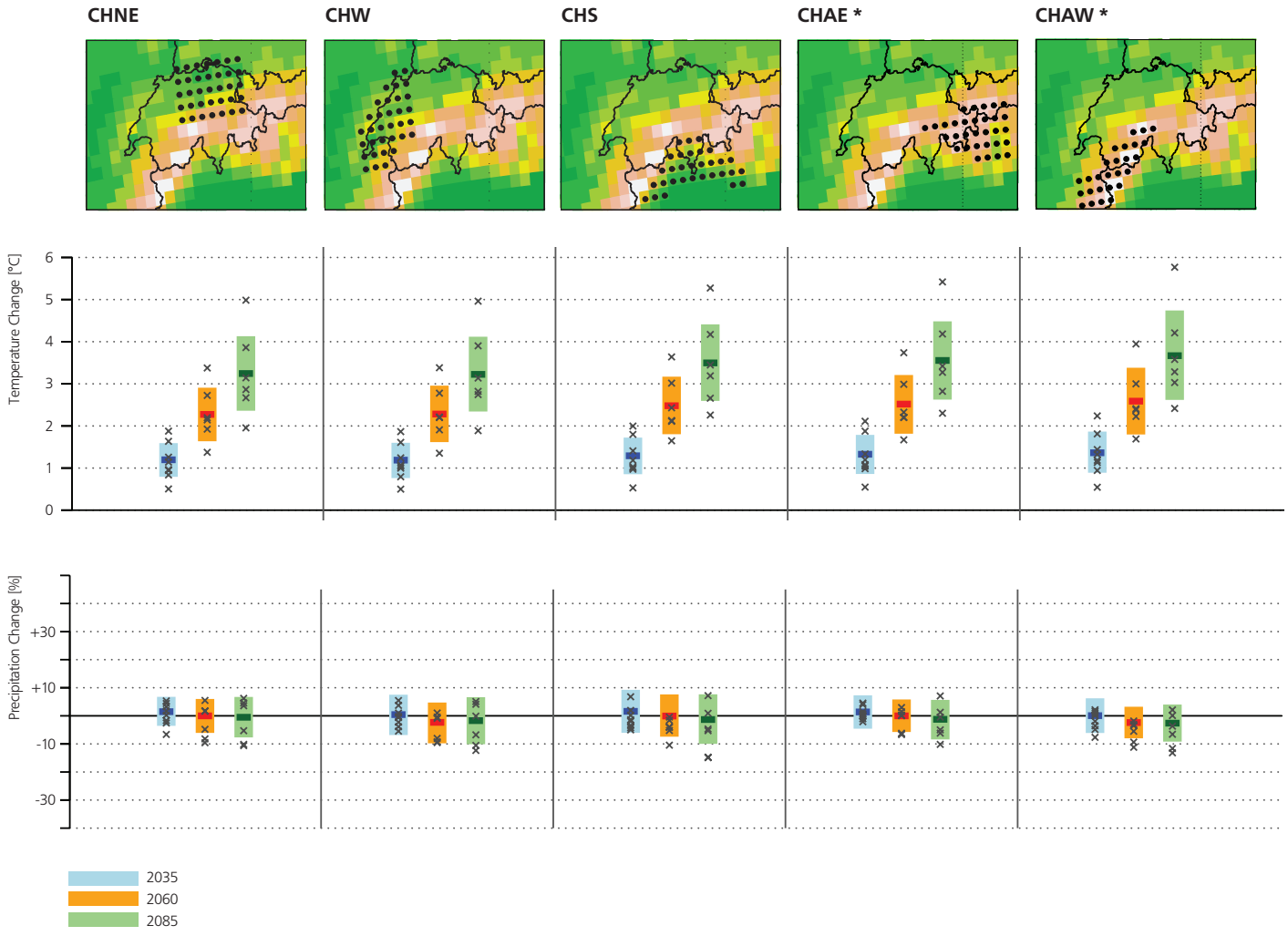

4| Continuous climate scenarios for the 21st century

For impact applications that slowly respond to temperature increases such as for instance mountain glaciers (e.g. VAW 2011; Huss 2012), climate scenarios in a continuous manner are more helpful than static snapshots of changes (Tebaldi and Sanso 2009; Harris et al. 2010). This would also help to inspect the (non-)linearity of temporal changes and to better detect emerging differentiations across emission scenarios, regions or seasons.

In order to provide temperature and precipitation change scenarios in a quasi-transient manner across the 21st century, we apply our multi-model combination algorithm to 10 additional future scenario periods. These additional (overlapping) 30year-periods are chosen, so that the entire 21st century is covered (from 2005 to 2099). The central years of the periods are consecutively shifted by five years starting from 2020 until 2085.

Figure 3 displays the modeled seasonal temperature and precipitation changes over northeastern Switzerland for all considered periods. In general, the regional warming signals in the models enlarge over the century. Thereby, the overall spread across the models steadily increases, too. The ranking of model changes essentially depends on the model's regional temperature sensitivity to the specified amount of greenhouse gas concentration according to the A1B emission scenario. This amount remains relatively invariant from season to season and from scenario period to scenario period. Note, that the model ranking is used in a concurrent extension article that analyzes inter-variable and inter-seasonal dependencies in the CH2011 scenarios (Fischer et al. 2016).

In case of precipitation, the ranking of modeled changes is less well established, varying from season to season but also across lead-time of the same season (Figure 3). Much of these model response fluctuations appear to be random and not systematic. In fact, they are likely influenced by internal decadal variability (see «Fraction of internal decadal variability», p. 11). One exception is the summer season when an anthropogenic signal clearly emerges with a decreasing trend in all of the models. This process increases over lead-time in all of the models, thereby contributing to a model ranking that stays similar from period to period.

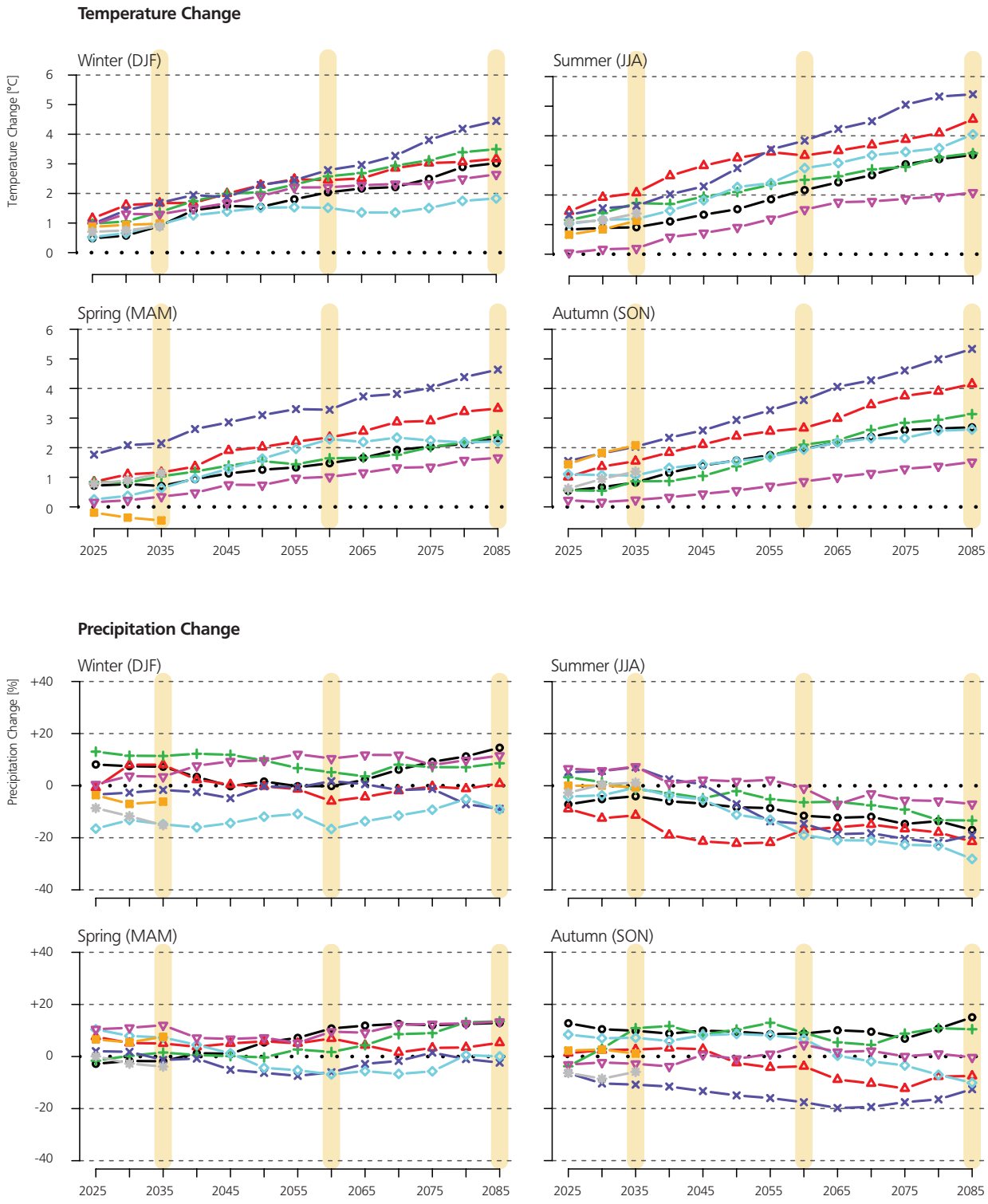

Figure 3

Expected changes in seasonal mean temperature (in °C) and seasonal mean precipitation (in %) as projected by the set of climate models used in CH2011 (2011) for the A1B emission scenario and the region CHNE. Shown are 30 year average changes across the 21st century with respect to 1980–2009, plotted at the central year of time period. The colored lines represent the model-simulated changes at each scenario period, that serve as input to the multi-model combination algorithm (RCM simulations driven by the same GCM are averaged beforehand). Note that two models only cover the first three periods (up to 2035). The vertical orange bars indicate those time periods that were subject to multi-model combination in CH2011.

Combined multi-model projections

The combined multi-model projections with upper and lower estimates are shown at the example of northeastern Switzerland in Figure 4. For the A1B emission scenario, temperature over Switzerland is projected to increase almost linearly over the century.

The range of uncertainty slightly increases with lead-time, particularly in summer. In contrast, the expected changes following the RCP3PD scenario level off at around 2040 and, from then on, become distinguishable from the changes at A1B. The projections according to A2 emerge from the ones of A1B only after 2060, following the applied pattern-scaling factors (Fischer et al. 2012). Common to all evaluated temperature projections over the 21st century is a clear temperature deviation from reference climate.

From autumn to spring, the multi-model combination does not favor precipitation changes over Switzerland of a particular sign throughout the 21st century and in any of the emission scenarios. The uncertainty range largely depends on region and season. The only tendency that can be inferred for the A1B and A2 scenario is an increase in winter precipitation over CHS and CHAE that begins to deviate from RCP3PD at around the middle of the century (not shown).

In contrast, summer precipitation, according to A1B and A2, begins to steadily decrease from 2040 onwards, related to a large-scale summer drying over Southern Europe and France, that also becomes dominant over Switzerland (Rowell and Jones 2006; Fischer et al. 2012). Around 2050 summer precipitation deviates significantly from the reference climate, first in the westerly located regions (CHW and CHAW) and at around 2060 over the regions CHNE, CHAE and CHS. Projections following the RCP3PD emission scenario decrease less steeply, but deviations from today's precipitation mean amounts are still expected.

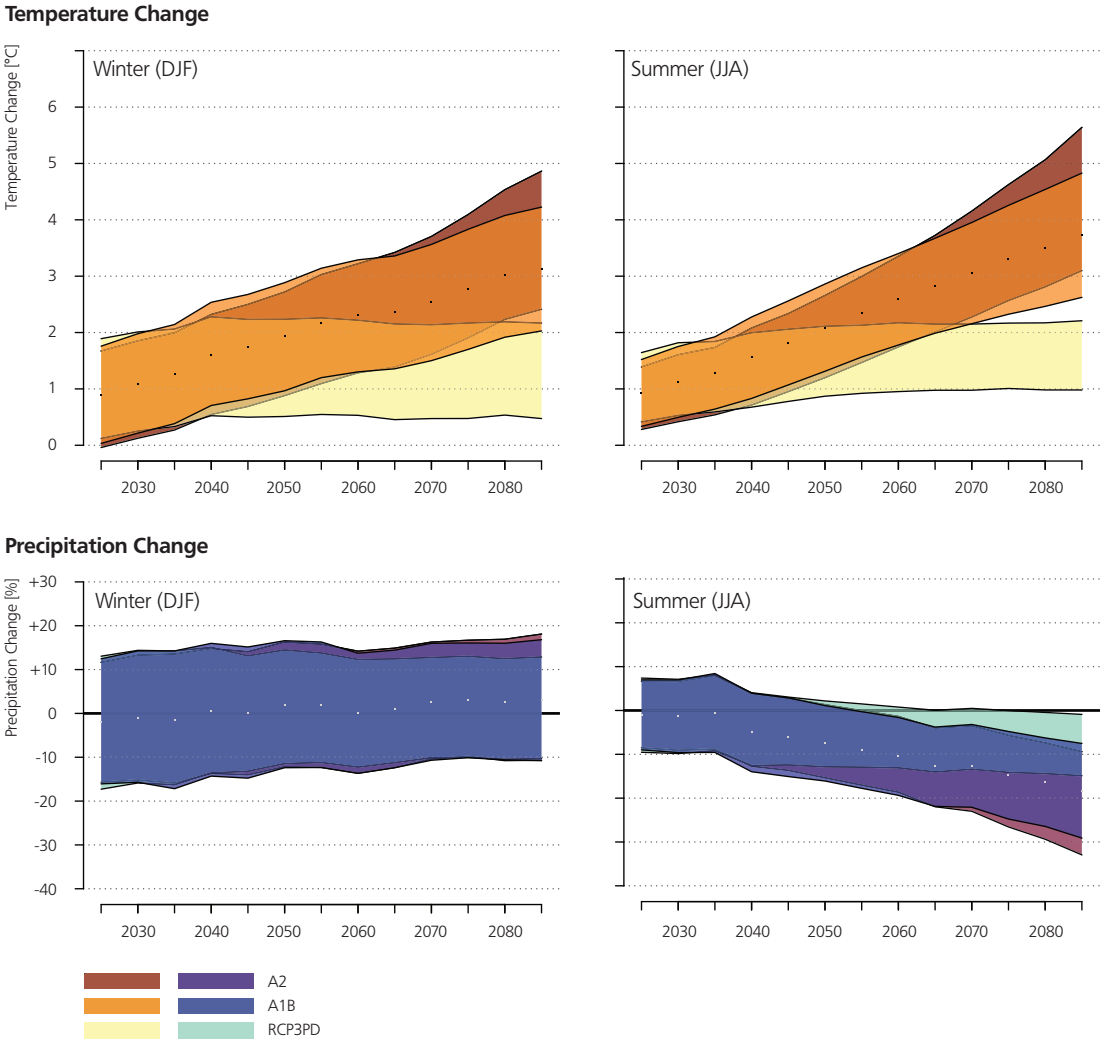

Figure 4
Projected future changes of temperature (upper panel, in °C) and relative precipitation (lower panel, in %) for winter and summer and according to the three emission scenarios (A1B, A2, RCP3PD). Shown are the upper and lower estimates of a sliding 30 year time-period over the 21st century. The changes are relative to the mean over 1980-2009 and representative for northeastern Switzerland (i.e., CHNE). Projections for the A1B emission scenario are assessed with the Bayesian multi-model combination algorithm, while those of A2 and RCP3PD are scaled based on global mean temperature change. The dots in the plots represent the medium estimates following the A1B scenario.

Fraction of internal decadal variability

The projections of Figure 4 are the result of the joint assessment of several climate model projections (model uncertainty) and the inclusion of observed internal decadal variability. Here, it is our aim to quantify the proportion of internal decadal variability (in %) in the disseminated climate scenarios of seasonal means at A1B. Whereas the internal decadal variability is inherent to the climate system, the model uncertainty – to a limited extent – might be reduced by future model improvements. Different to a similar study by Hawkins and Sutton (2009; 2010), we do not additionally analyze fractional uncertainties arising from the choice of emission scenario. This is because our projections for A2 and RCP3PD scenarios are not explicitly run by climate models, but linearly scaled based on global mean temperature (Fischer et al. 2012). For methodological details on the separation of model uncertainty and internal decadal variability, we refer to Appendix A3.

The analysis reveals, that the relative fractions of the two components, i.e. internal decadal variability and model uncertainty, are heavily dependent on the chosen variable, season and lead-time. This is illustrated in Figure 5 at the example of northeastern Switzerland for both temperature and precipitation changes. Generally, the fraction of internal decadal variability is smaller in summer compared to winter and it is smaller for temperature than for precipitation. The opposite is true regarding model uncertainty. A further obvious characteristic is that the relative fractions do not necessarily stay constant over lead-time. In fact, for temperature and summer precipitation, the proportions of model uncertainty are increasing with lead-time at the expense of internal variability. This is because the modeled changes deviate more and more from each other (Figure 3), while internal decadal variability does not change in absolute terms. Therefore, in relative terms, internal variability is generally largest for the earliest periods and decreases towards the end of the century. As can be seen in Figure 5, internal decadal variability contributes to roughly half of the uncertainty spread in winter temperature changes at 2025, but shrinks to less than 30% toward the end of the century. Similarly, for summer temperature and summer precipitation the contributions are marked by a continuous decrease from around 30% in 2025 down to around 10–20% in 2085.

In cases where the modeled changes keep fluctuating around zero without any multi-model mean tendencies (see Figure 3), internal decadal variability generally explains a much bigger part of the uncertainty throughout the 21st century. This is for instance the case for precipitation projections from autumn until spring in northeastern Switzerland. During winter, internal decadal variability amounts to about 40% in relative terms and stays at this level until the end of the century (Figure 5). This means that even for the farthest lead-times, precipitation projections over Switzerland are affected to a large degree by pure internal variability, for instance caused by variability in synoptic circulation over central Europe (van Ulden and van Oldenborgh 2006).

Figure 5

Relative fractions of internal decadal variability (grey, in %) and model uncertainty (red, in %) to the projection uncertainty of the A1B scenario as displayed in Figure 4. Shown are the proportions for the northeastern region of Switzerland (CHNE) over the 21st century. The upper (lower) panels display the fractions for temperature (precipitation) changes.

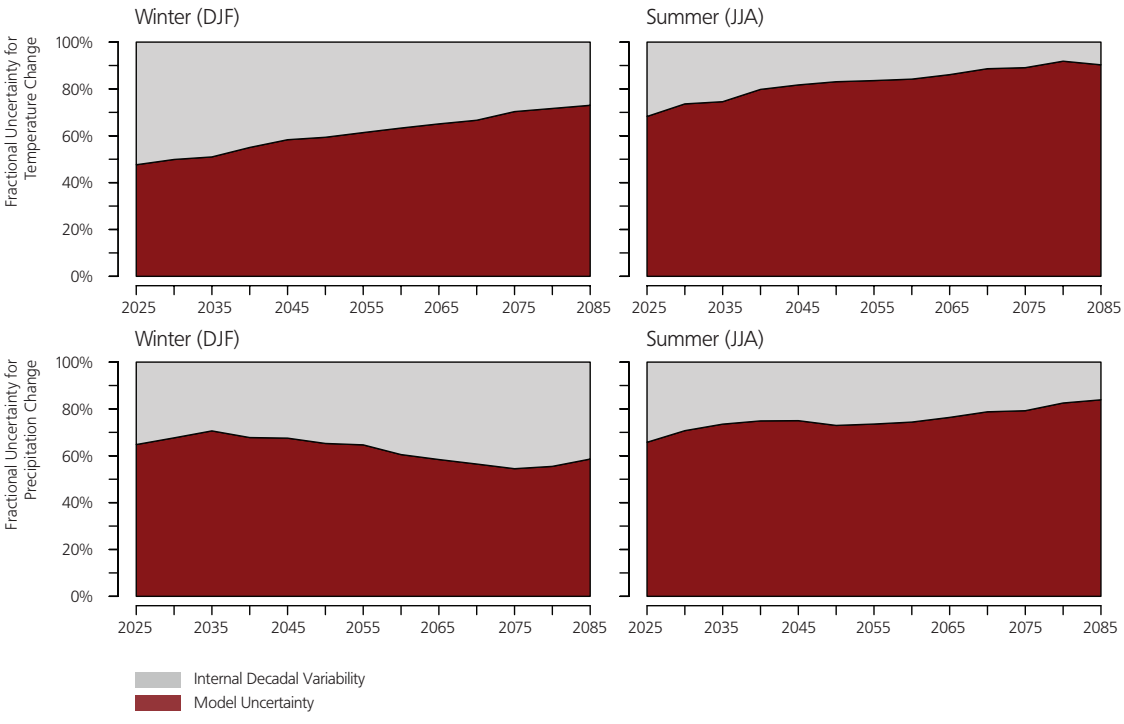

5| Conclusions and Implications for End-Users

This study extends the joint multi-model assessment of CH2011 to new regions covering the Alps, additional scenario periods and to annual averages. All of these extended assessments were based on the same climate model data and the same statistical post-processing techniques as in CH2011. This includes the same conceptual assumptions as in CH2011 (2011; see Appendix A1 therein). Our results are consistent with the data and knowledge at hand but several findings are subject to uncertainties and may change with future model generations and larger model sample sizes becoming available.

Our main findings on the new extended projections can be summarized as:

1 Toward the end of the century temperature is expected to increase slightly stronger over the newly analyzed regions of higher elevation compared to the regions north and south of the Alps. For the A2 scenario, the medium estimates over CHAW and CHAE indicate a warming of around 3.7–5.3°C depending on season. In contrast, for the mitigation scenario RCP3PD, these estimates amount to only around 1.4–2°C.

2 Precipitation projections over the Alps show similar tendencies as over the lower elevated regions assessed in CH2011 (2011). For the A2 scenario, the medium estimates indicate a decrease in summer precipitation over CHAE of around 15% and over CHAW of around 23% toward the end of the century. For the mitigation scenario RCP3PD, these estimates lie at around 6% and 8%, respectively.

3 If greenhouse gas emissions evolve as in the A2 scenario, annual average temperatures over Switzerland are expected to increase by around 3.8–4.3°C by 2085 (medium estimates) depending on region. Following the mitigation scenario RCP3PD, temperatures will rise less strongly: in the mean by only about 1.4–1.6°C. The annual average changes in temperature are close to arithmetic averages over the four, separately assessed, seasonal changes of CH2011.

4 For annual mean precipitation, no common sign of change can be inferred over Switzerland. Projected medium estimates are close to zero throughout the 21st century with uncertainty ranges bounded by maximum -12% and +9%. The uncertainty ranges for annual precipitation changes are far smaller than those of seasonal mean changes presented in CH2011. Annual mean temperature changes and associated uncertainties are comparable to values derived from an arithmetic average over all seasons.

5 Temperature mean changes evolve almost linearly over the century for the A1B scenario, while projections following the A2 scenario emerge from those of A1B only after 2060. Expected changes according to the RCP3PD scenario level off at around 2040.

6 Throughout the century, no common sign of change is projected by the multi-model set regarding winter, spring and fall precipitation, except for an increasing tendency in winter precipitation over the southerly located regions CHS and CHAE (A1B and A2 scenario). In summer, it is expected that precipitation declines earlier and stronger in the westerly located regions (CHW and CHAW) compared to the rest of Switzerland.

7 Internal decadal variability represents an important contributor to uncertainty in the CH2011 climate scenarios of seasonal means. In relative terms, its proportion shrinks markedly over the century regarding temperature and summer precipitation projections. For precipitation changes in winter, spring and autumn in northeastern Switzerland, internal decadal variability remains large, with a magnitude of around 40% throughout the century.

6| Overview of datasets and terms of use

The following new datasets are available from www.ch2011.ch:

- Climate scenarios of seasonal means over the Alpine regions «CHAW» and «CHAE», version 2.0 (Described in Section 2)
- Climate scenarios of annual averages (Described in Section 3)
- Continuous climate scenarios of seasonal means for the entire 21st century (Described in Section 4)

References

Begert, M., T. Schlegel, and W. Kirchoffer, 2005: Homogeneous temperature and precipitation series of Switzerland from 1864 to 2000, *International Journal of Climatology,* **25,** 65-80, doi: 10.1002/joc.1118.

Bosshard, T., S. Kotlarski, T. Ewen, and C. Schär, 2011: Spectral representation of the annual cycle in the climate change signal, *Hydrology and Earth System Sciences,* **15,** 2777-2788, doi: 20.5194/hess-15-2777-2011.

Buser, C. M., H. R. Künsch, D. Lüthi, M. Wild, and C. Schär, 2009: Bayesian multi-model projection of climate: bias assumptions and interannual variability, *Climate Dynamics,* **33,** 849-868, doi: 10.1007/s00382-009-0588-6.

CH2011, 2011: Swiss Climate Change Scenarios CH2011, published by C2SM, MeteoSwiss, ETH, NCCR Climate, and OcCC, Zurich, Switzerland, 88 pp. ISBN: 978-3-033-03065-7.

Fischer, A. M., A. P. Weigel, C. M. Buser, R. Knutti, H. R. Künsch, M. A. Liniger, C. Schär, and C. Appenzeller, 2012: Climate change projections for Switzerland based on a Bayesian multi-model approach, *International Journal of Climatology,* **32,** 15, 2348-2371, doi: 10.1002/joc.3396.

Fischer, A. M., D. E. Keller, M. A. Liniger, J. Rajczak, C. Schär, and C. Appenzeller, 2014: Expected future changes in precipitation intensity and frequency in Switzerland: a multi-model perspective *International Journal of Climatology,* doi: 10.1002/joc.4162.

Fischer, A. M., M. A. Liniger, and C. Appenzeller, 2016: Climate scenarios of seasonal means: inter-variable and inter-seasonal correlations, *CH2011 Extension Series No. 3,* Zurich, in press.

FOEN, 2012: Effects of Climate Change on Water Resources and Waters Synthesis report on «Climate Change and Hydrology in Switzerland», *Federal Office for the Environment FOEN,* Berne, Switzerland.

Harris, G. R., M. Collins, D. M. H. Sexton, J. M. Murphy, and B. B. B. Booth, 2010: Probabilistic projections for 21st century European climate, *Nat. Hazards Earth Syst. Sci.,* **10,** 2009-2020, doi: 10.5194/nhess-10-2009-2010.

Hawkins, E., and R. Sutton, 2009: The potential to narrow uncertainty in regional climate predictions, *Bulletin of the American Meteorological Society,* **90,** 1095-1107.

Hawkins, E., and R. Sutton, 2010: The potential to narrow uncertainty in projections of regional precipitation change, *Climate Dynamics,* **37,** 1-12, doi: 10.1007/s00382-010-0810-6.

Haylock, M. R., N. Hofstra, A. M. G. Klein Tank, E. J. Klok, P. D. Jones, and M. New, 2008: A European daily high-resolution gridded data set of surface temperature and precipitation for 1950-2006, *Journal of Geophysical Research-Atmospheres,* **113,** D20119, doi: 10.1029/2008JD010201.

Huss, M., 2012: Extrapolating glacier mass balance to the mountain-range scale: the Europen Alps 1900-2100, *The Cryosphere,* **6,** 713-727, doi: 10.5194/tc-6-713-2012.

Im, E. S., E. Coppola, F. Giorgi, and X. Bi, 2010: Local effects of climate cange over the Alpine region: A study with a high resolution regional cliamte model with a surrogate climate change scenario, *Geophysical Research Letters,* **37,** L05704, doi: 10.1029/2009GL041801.

Knutti, R., R. Furrer, C. Tebaldi, J. Cermak, and G. A. Meehl, 2010: Challenges in Combining Projections from Multiple Climate Models, *Journal of Climate,* **23,** 2739-2758, doi: 10.1175/2009JCLI3361.1.

Kotlarski, S., T. Bosshard, D. Lüthi, P. Pall, and C. Schär, 2012: Elevation gradients of European climate change in the regional cliamte mdoel COSMO-CLM, *Climatic Change,* **112,** 189-215, doi: 10.1007/s10584-011-0195-5.

Nakicenovic, N. and R. Swart, 2000: IPCC Special Report on Emissions Scenarios, Cambridge, UK and New York, NY, USA.

Rowell, D. P., and R. G. Jones, 2006: Causes and uncertainty of future summer drying over Europe, *Climate Dynamics,* **27,** 281-299, doi: 10.1007/s00382-006-0125-9.

Tebaldi, C., and B. Sanso, 2009: Joint projections of temperature and precipitation change from multiple climate models: a hierarchical Bayesian approach, *J. R. Statist. Soc. A.,* **172,** 83-106.

Van Ulden, A. P., and G. J. van Oldenborgh, 2006: Large-scale atmospheric circulation biases and changes in global climate model simulations and their importance for climate change in Central Europe. *Atmospheric Chemistry and Physics,* **6,** 863-881.

VAW 2011: Veränderung der Gletscher und ihrer Abflüsse 1900-2100 - Fallstudien Gornergletscher und Mattmark, *VAW,* Zurich, Mai 2011.

Zubler, E. M., A. M. Fischer, M. A. Liniger, M. Croci-Maspoli, S. C. Scherrer, and C. Appenzeller, 2014: Localized climate change scenarios of mean temperature and precipitation over Switzerland, *Climatic Change,* **125,** 237-252, doi: 10.1007/s10584-014-1144-x.

Technical Appendix

A1 Uncertainty framework of CH2011

Climate projections are inherently associated with a cascade of uncertainties, especially on regional scales such as Switzerland. These include uncertainty about the future evolution of greenhouse gas concentrations, uncertainty arising from multiple climate model projections, and internal decadal variability (Knutti et al. 2010). To quantify climate change uncertainty in CH2011 (2011), a sophisticated multi-model combination algorithm (Bayesian algorithm by Buser et al. 2009; in the following referred to as «BAB») was employed to the seasonally and regionally aggregated model output of ENSEMBLES at the A1B emission scenario. The BAB combines observational data with model data for past and future climatic conditions yielding projections of the «true» climate shift *(«Δμ»)* in form of a probability distribution function (PDF). In practice, the algorithm comes with a number of pre- and post-processing steps (before and after multi-model combination), that are described in detail in Fischer et al. (2012). As a final outcome, PDFs of the climate shift are obtained that include uncertainty from model projections and internal decadal variability for a specific region, season and pair of scenario-reference period.

Here, we briefly recapitulate those methodological challenges in the CH2011 scenario production that are also of relevance for extending the scenario database to new regions, annual averages, and to new scenario periods.

1 Prior to multi-model combination with the BAB, it has to be checked if the model and observational input data are normally distributed. This is a pre-requirement of the BAB. For the seasonal precipitation amounts in CH2011 this preconditioning can be met by transforming the input data with a square root function (Fischer et al. 2012). The same transformation is applied to seasonal precipitation averages over the Alpine regions and to those at new future periods. In case of annual precipitation amounts, though, it turns out that these aggregated data are already sufficiently normally distributed, so that a transformation can be omitted.

2 Another challenge is the specification of an important prior assumption of how much model projections are allowed to diverge from each other with lead-time. Restricting this divergence to a very small range results in a PDF of climate change *(Δμ)* that is very sharp. Choosing a very wide range a priori transforms into a PDF of Δμ with only very little information (Buser et al. 2009). To pragmatically solve this dilemma, the range of allowed model deviation is investigated and determined with the help of the raw model projections themselves. In particular, the spread of the projected changes (similar to Figure 3) is quantified with the sample variance separately for different lead-times (Fischer et al. 2012). For the scenario extensions to additional future periods, this prior assumption has to be iteratively determined for each further lead-time period.

3 The BAB itself is not designed to handle internal decadal variability. Therefore, Fischer et al. (2012) proposed a way to circumvent the presence of internal decadal variability during the multi-model combination step by the BAB. Specifically, the variability component is removed statistically from the BAB's input data of model projections and observations following the procedure outlined in Hawkins and Sutton (2009). After multi-model combination the resulting PDF of Δμ is inflated again with internal decadal variability. As Δμ describes the «true» future shift in relation to a reference period, we inflate the PDF with observed decadal variability. The latter is derived from long-term observation measurements at individual stations over Switzerland (see below).

4 The resulting confidence intervals of a quantity change (for a given lead-time, season and region), as for instance shown in Figure 1, are finally subject to an expert judgment, advising not to interpret the PDF in a strict probabilistic way. Rather, the 2.5th, 50th and 97.5th percentiles are considered as three possible outcomes of future climate (disseminated as a lower, medium and upper estimate) with no explicit probability statement being made. The reason is that the underlying model ensemble in CH2011 should be regarded as an ensemble of opportunity that may or may not sample the full range of model uncertainty (Knutti et al. 2010).

A2 Scenario Calculations for the new Alpine regions CHAE and CHAW

The choice of grid-points for the two additional regions «CHAE» and «CHAW» is based on several prerequisites. First, the regions should not overlap with each other, should include a similar number of grid-points (due to sampling issues) and taking all CH2011 regions together, they should fully cover the territory of Switzerland. Second, each region should be climatologically homogenous with respect to long-term trends and interannual variability. To assess the latter requirement on a semi-empirical basis, we inspect grid-point correlations to a core region, which is subjectively determined beforehand. On the basis of the spatial grid-point correlations surrounding the core region, grid points of similar climatological characteristics can be identified and are selected for the region of interest (for more details we refer to section 2.3 in Fischer et al. 2012). As the topography varies from model to model, we investigate correlations in each model separately and compare the results with those from gridded observations (Haylock et al. 2008). Since the obtained correlations are seasonally dependent, the choice of spatial extent ultimately remains a (subjective) compromise between different requirements.

To include observed internal decadal variability in the scenario calculations over these new regions, we select the mean of measurements for «Chateau d'Oex», «Sils Maria» and «Davos» as representative observation for both regions. This approach differs from Zubler et al. (2014), who selected the mean of measurements for «Chateau d'Oex» and «Grand-St. Bernhard» for CHAW and the mean for «Sils Maria» and "Davos» for CHAE. Over complex topography the selection of observations strongly matters. Here, we argue that the chosen set of Alpine stations in Zubler et al. (2014) is not optimal, as it results in a considerably reduced estimate in internal decadal variability of relative precipitation for CHAW compared to CHAE. This, however, is likely not physically-based, but methodologically related. The difference in variability occurs because for CHAW, both «Chateau d'Oex» and «Grand-St. Bernhard» are rather high-elevated stations with rather large absolute precipitation amounts, but with low variability in relative terms. On the contrary, for CHAE, «Sils Maria» lies in an Alpine valley and therefore exhibits rather low absolute precipitation amounts throughout the year, but high variability in relative terms. Another reason for the rather large difference in internal variability between CHAE and CHAW is a different time-window used for the analysis: for observations over CHAW, due to data quality issues for «Grand-St. Bernhard», only a reduced time-window (back to 1919) is taken into account in Zubler et al. (2014). In case of relative precipitation, the reduced time-window reduces the amount of estimated internal decadal variability considerably and also leaves a signature on the uncertainty range spanned between upper and lower estimates in precipitation.

From a physical point of view, it is not obvious why the two regions should be subject to different internal variabilities. There is also no indication from model simulations that would support this difference. Therefore, to circumvent the methodological issue, we use the internal variability estimated from the same set of station observations (i.e., «Chateau d'Oex», «Sils Maria» and «Davos») for both regions, CHAE and CHAW. The three stations feature rather different climatological characteristics and cover the full instrumental measurement period back to 1864 (Begert et al. 2005).

To what degree do the two versions of Alpine scenario datasets differ? Comparing precipitation changes of version 2.0 (proposed in this article) to version 1.0 (of Zubler et al. 2014) reveals at all lead-times in general larger uncertainty ranges in version 2.0 for the region CHAW and slightly smaller ranges for the region CHAE. Most markedly, the upper/lower estimates of version 2.0 exceed the ones of version 1.0 over CHAW by around +/-4% for DJF and by around +/-8% for MAM. The medium estimates in the two versions stay at around the same level. Regarding temperature changes, the differences between the two versions are minor: version 2.0 features a somewhat enlarged uncertainty range over both regions, especially for MAM (upper/lower estimates of version 2.0 exceed the ones of version 1.0 by around +/-0.2°C).

A3 Fraction of internal decadal variability

To quantify the proportion of internal decadal variability to the disseminated uncertainty ranges of the CH2011 scenarios (as for instance presented in Figure 1), we inter-relate the uncertainty in the obtained PDFs of climate change ($\Delta\mu$, from the BAB), prior to the inflation with internal decadal variability ($\Delta\mu^{model}$) and afterwards ($\Delta\mu^{model+IDV}$). Specifically, the ratio of the standard deviations is used as a measure of the relative fraction (*i.e.*, $sdev\langle\Delta\mu^{model}\rangle / sdev\langle\Delta\mu^{model+IDV}\rangle$). Taking advantage of the new transient scenarios (Section 4), this ratio is calculated at each lead-time, region and season, separately.

A4 Tables of seasonal probabilistic estimates for the Alpine regions CHAE and CHAW

Temperature Change

Table A1
Values of projected future seasonal temperature change (in °C) as shown with colored bars in Figure 1 for the A1B emission scenario. The estimates for 2035, 2060 and 2085 refer to the 30-year intervals 2020–2049, 2045–2074, and 2070–2099. Reference period is 1980–2009. Note, that these estimates are based on version 2.0 of the seasonal mean scenarios over the Alps and differ to those of Zubler et al. (2014).

			2035			2060			2085		
Region	Season	Scen	Lower	Med	Upper	Lower	Med	Upper	Lower	Med	Upper
CHAE	DJF	A2	0.59	1.21	1.83	1.63	2.47	3.32	2.8	4.01	5.28
		A1B	0.7	1.35	2	1.67	2.52	3.38	2.38	3.44	4.56
		RCP3PD	0.64	1.28	1.92	0.88	1.51	2.15	0.84	1.46	2.11
	MAM	A2	0.13	0.92	1.72	1.25	2.2	3.17	2.45	3.71	4.98
		A1B	0.2	1.03	1.87	1.28	2.25	3.23	2.06	3.19	4.31
		RCP3PD	0.17	0.97	1.79	0.6	1.35	2.11	0.62	1.36	2.09
	JJA	A2	0.62	1.31	2	1.97	2.85	3.73	3.6	4.79	6
		A1B	0.74	1.47	2.19	2.02	2.91	3.8	3.05	4.11	5.19
		RCP3PD	0.68	1.39	2.1	1.05	1.74	2.43	1.09	1.75	2.43
	SON	A2	0.69	1.25	1.8	1.47	2.31	3.16	2.65	3.95	5.19
		A1B	0.8	1.4	2	1.5	2.36	3.22	2.26	3.39	4.47
		RCP3PD	0.74	1.33	1.9	0.83	1.41	1.99	0.87	1.44	1.99
CHAW	DJF	A2	0.57	1.17	1.8	1.55	2.41	3.26	2.71	3.94	5.18
		A1B	0.68	1.32	1.97	1.59	2.46	3.33	2.3	3.38	4.47
		RCP3PD	0.62	1.25	1.89	0.83	1.47	2.11	0.82	1.44	2.08
	MAM	A2	0.11	0.91	1.7	1.09	2.16	3.2	2.21	3.7	5.18
		A1B	0.19	1.02	1.84	1.13	2.2	3.26	1.85	3.17	4.49
		RCP3PD	0.15	0.97	1.77	0.49	1.32	2.12	0.55	1.35	2.16
	JJA	A2	0.74	1.48	2.23	2.24	3.22	4.22	3.89	5.35	6.75
		A1B	0.88	1.67	2.46	2.29	3.29	4.3	3.31	4.59	5.82
		RCP3PD	0.81	1.57	2.34	1.22	1.97	2.71	1.23	1.95	2.7
	SON	A2	0.67	1.26	1.85	1.44	2.36	3.28	2.69	4.05	5.41
		A1B	0.77	1.41	2.05	1.47	2.41	3.35	2.28	3.47	4.65
		RCP3PD	0.72	1.34	1.95	0.81	1.44	2.06	0.89	1.48	2.07

Precipitation Change

Table A2
Values of projected future seasonal precipitation change (in %) as shown with colored bars in Figure 1 for the A1B emission scenario. The estimates for 2035, 2060 and 2085 refer to the 30-year intervals 2020–2049, 2045–2074, and 2070–2099. Reference period is 1980-2009. Note, that these estimates are based on version 2.0 of the seasonal mean scenarios over the Alps and differ to those of Zubler et al. (2014).

			2035			2060			2085		
Region	Season	Scen	Lower	Med	Upper	Lower	Med	Upper	Lower	Med	Upper
CHAE	DJF	A2	-13.3	0.6	14	-10.1	4.3	19.9	-5.9	10.3	26.9
		A1B	-13.7	0.7	14.4	-10.1	4.3	20.1	-6.4	8.8	24.4
		RCP3PD	-13.5	0.6	14.2	-10.5	2.5	16.2	-9	3.8	16.4
	MAM	A2	-14.5	0.8	16.3	-16.2	-0.8	14.4	-17.3	-0.8	15.7
		A1B	-14.6	0.8	16.7	-16.2	-0.8	14.4	-16.8	-0.7	15.2
		RCP3PD	-14.5	0.8	16.5	-15.3	-0.6	14.3	-15	-0.4	14.3
	JJA	A2	-6	0.4	6.8	-11.8	-6.3	-0.7	-23.3	-15.3	-7
		A1B	-6.5	0.4	7.4	-11.9	-6.5	-0.8	-20.2	-13.1	-5.8
		RCP3PD	-6.2	0.4	7.1	-8.2	-3.9	0.5	-10	-5.6	-1.1
	SON	A2	-9.9	0.6	11.1	-15.1	-1	13.4	-23.2	-5.4	13.5
		A1B	-10.4	0.7	11.8	-15.3	-1.1	13.7	-20.4	-4.6	12.1
		RCP3PD	-10.1	0.6	11.5	-11.2	-0.5	10.1	-11.7	-1.9	8
CHAW	DJF	A2	-16.2	-1	14.1	-14	0	14.4	-13.1	2.3	17.8
		A1B	-16.9	-1.2	14.7	-14.1	0	14.4	-12.6	2	16.6
		RCP3PD	-16.5	-1.1	14.4	-12.9	0	13.1	-11.8	0.9	13.3
	MAM	A2	-16.6	-1	14.7	-18.9	-3.7	11.4	-20.8	-4.1	12.4
		A1B	-17.1	-1	14.8	-19	-3.8	11.3	-19.6	-3.5	12.4
		RCP3PD	-16.9	-1	14.8	-17.1	-2.2	12.4	-16.3	-1.4	13.1
	JJA	A2	-8.6	-1.2	6.3	-19.2	-12.8	-6.1	-31.8	-23	-14.1
		A1B	-9.4	-1.4	6.9	-19.5	-13.1	-6.2	-27.5	-19.7	-11.9
		RCP3PD	-9	-1.3	6.5	-12.6	-7.8	-2.9	-13	-8.4	-3.9
	SON	A2	-13.4	-2.9	7.7	-18.3	-5.9	6.3	-24.4	-9.5	5.7
		A1B	-14.3	-3.2	8	-18.6	-6	6.3	-21.6	-8.2	5.4
		RCP3PD	-13.9	-3	7.9	-13.5	-3.6	6.1	-12.7	-3.5	5.8

A5 Tables of probabilistic estimates of annual averaged changes

Table A3

Values of projected future annual temperature change (in °C) as shown with colored bars in Figure 1 for the A1B emission scenario. The estimates for 2035, 2060 and 2085 refer to the 30-year intervals 2020–2049, 2045–2074, and 2070–2099. Reference period is 1980–2009.

Temperature Change

		2035			2060			2085		
Region	Scen	Lower	Med	Upper	Lower	Med	Upper	Lower	Med	Upper
CHNE	A2	0.69	1.06	1.44	1.6	2.22	2.86	2.76	3.78	4.79
	A1B	0.79	1.19	1.6	1.63	2.27	2.92	2.36	3.24	4.11
	RCP3PD	0.74	1.13	1.52	0.94	1.36	1.77	0.97	1.38	1.79
CHW	A2	0.67	1.06	1.45	1.56	2.24	2.89	2.74	3.76	4.79
	A1B	0.76	1.19	1.61	1.6	2.28	2.95	2.34	3.23	4.12
	RCP3PD	0.72	1.13	1.53	0.92	1.37	1.81	0.95	1.37	1.81
CHS	A2	0.75	1.15	1.56	1.78	2.44	3.1	3.03	4.08	5.14
	A1B	0.86	1.29	1.74	1.82	2.49	3.16	2.59	3.5	4.41
	RCP3PD	0.81	1.22	1.65	1.05	1.49	1.92	1.07	1.49	1.92
CHAE	A2	0.76	1.18	1.61	1.78	2.47	3.15	3.06	4.14	5.24
	A1B	0.86	1.33	1.79	1.82	2.52	3.22	2.62	3.55	4.5
	RCP3PD	0.81	1.25	1.7	1.04	1.51	1.98	1.05	1.52	1.99
CHAW	A2	0.77	1.22	1.66	1.75	2.53	3.31	3.07	4.28	5.51
	A1B	0.89	1.37	1.84	1.79	2.59	3.38	2.62	3.67	4.75
	RCP3PD	0.83	1.3	1.75	1.03	1.55	2.07	1.06	1.56	2.09

Table A4

Values of projected future annual precipitation change (in %) as shown with colored bars in Figure 1 for the A1B emission scenario. The estimates for 2035, 2060 and 2085 refer to the 30-year intervals 2020–2049, 2045–2074, and 2070–2099. Reference period is 1980–2009.

Precipitation Change

		2035			2060			2085		
Region	Scen	Lower	Med	Upper	Lower	Med	Upper	Lower	Med	Upper
CHNE	A2	-3.8	1.3	6.3	-6	-0.1	5.9	-8.9	-0.7	7.5
	A1B	-3.9	1.5	6.8	-6.1	-0.1	5.9	-7.8	-0.5	6.7
	RCP3PD	-3.8	1.4	6.5	-4.6	-0.1	4.6	-4.6	-0.2	4.2
CHW	A2	-6.4	0.4	7.3	-9.4	-2.3	4.8	-11.1	-2	7.2
	A1B	-6.6	0.4	7.5	-9.5	-2.4	4.8	-10.1	-1.7	6.8
	RCP3PD	-6.5	0.4	7.4	-7.9	-1.4	5	-7.5	-0.7	5.9
CHS	A2	-5.9	1.4	8.7	-7.3	-0.1	7.3	-11.3	-1.5	8.2
	A1B	-6.1	1.6	9.3	-7.4	-0.1	7.4	-10.1	-1.3	7.5
	RCP3PD	-6	1.5	9	-6.1	0	6.1	-6.7	-0.5	5.5
CHAE	A2	-4.4	1.3	7.1	-5.7	0	5.8	-9.2	-1.4	6.3
	A1B	-4.5	1.5	7.5	-5.7	0	5.9	-8.3	-1.2	5.7
	RCP3PD	-4.4	1.4	7.3	-5	0	5.1	-5.6	-0.5	4.6
CHAW	A2	-5.7	0	5.9	-8	-2.4	3.2	-10.5	-3.1	4.1
	A1B	-6	0	6.2	-8.1	-2.4	3.2	-9.4	-2.7	3.9
	RCP3PD	-5.8	0	6	-6.5	-1.5	3.5	-6.3	-1.2	3.8